Journal of Electroanalytical Chemistry 746 (2015) 25–30

Contents lists available at ScienceDirect

Journal of Electroanalytical Chemistry

journal homepage: www.elsevier.com/locate/jelechem

Electrolytic cell containing different groups of ions with anomalous diffusion approach

F.R.G.B. Silva [a], R. Rossato [a,b], E.K. Lenzi [a,c,*], R.S. Zola [a,b], H.V. Ribeiro [a,b], M.K. Lenzi [d], G. Gonçalves [e]

[a] Departamento de Física, Universidade Estadual de Maringá, Avenida Colombo 5790, 87020-900 Maringá, PR, Brazil
[b] Departamento de Física, Universidade Tecnológica Federal do Paraná, Rua Marcilio Dias 635, 86812-460 Apucarana, PR, Brazil
[c] Departamento de Física, Universidade Estadual de Ponta Grossa, Av. General Carlos Cavalcanti 4748, 84030-900 Ponta Grossa, PR, Brazil
[d] Departamento de Engenharia Química, Universidade Federal do Paraná, 81531-990 Curitiba, PR, Brazil
[e] Departamento de Engenharia Química, Universidade Tecnológica Federal do Paraná, Ponta Grossa 84016-210, PR, Brazil

ARTICLE INFO

Article history:
Received 11 October 2014
Received in revised form 19 March 2015
Accepted 19 March 2015
Available online 20 March 2015

Keywords:
Anomalous diffusion
Electrical response
Impedance

ABSTRACT

The electrical response of an electrolytic cell containing more than one group of ions is investigated under the fractional approach where integro – differential boundary conditions and fractional time derivative of distributed order are considered. The model derived here, which accounts for anomalous diffusion of charges in a dielectric media, is compared with experimental data for mixtures of two salts with same valence and water and a good agreement was found. We show that in the low frequency limit, the electrical response is essentially governed by the boundary conditions and suppress the formation of a second plateau predicted when surface effects are neglected, being therefore linked to an anomalous diffusive process which, in the usual circuit description, may be connected to constant phase elements. Our model may be important for the interpretation of ionic density measurements in liquid crystals and other electrolytic cells in a more realistic fashion.

1. Introduction

Comprehending the electrical response is an important issue since it plays a major role on the mechanism, kinetics, and thermodynamics of various physicochemical processes. In this context, the impedance spectroscopy [1] is an experimental technique of great popularity for analyzing the response of a system subjected to an external, usually of small amplitude, and periodic current signal. The results obtained via this technique have been investigated, in general, by the Poisson–Nernst–Planck (PNP) model and/or equivalent circuits. However, the behavior exhibited experimentally often deviate from what is obtained by the standard formalism, where the impedance Z assumes the asymptotic behavior $Z \sim 1/(i\omega)$ in the low frequency limit presented by the PNP model. This disagreement between experimental data and usual models is a strong motivation for considering changes in the usual description. One of them is concerned to the diffusive motion of the ions, which can be extended to anomalous diffusion, for instance, via fractional derivatives [2] or by generalizing the boundary conditions [3] due to the complexity of the surface effects. In fact, different scenarios have been considered with the fractional approach [4–7], including the description of electrolytic cells [8] with integro-differential boundary conditions (PNPA model) [9] taking into account surface effects that may lead to anomalous behavior such as the adsorption–desorption phenomena. The PNPA model has also been used to show that anomalous diffusion can indeed provide a new perspective to the investigation of electrical response [10,11], and that it can be connected with equivalent circuits with constant phase elements [12], having however, a deeper physical meaning. It is worth to point out that, electric circuits play an important role in the context of the electrical response. In particular, several arrangements of equivalent circuits have been proposed in agreement to experimental scenarios. An example is the Randles circuit [13] that consists of a resistance in series with a parallel combination of a double-layer capacitance and an impedance of a faradaic reaction which is also modified by incorporating constant phase elements. A detailed discussion about the various distributed circuit elements that can be incorporated into equivalent circuits was presented in Refs. [1,14–16]. However, as discussed in Ref. [17], it is necessary a careful analysis before reaching general conclusions about the data, since the incorrect choice of the equivalent circuit can lead to deceptive conclusions about the process that occurs in the cell.

* Corresponding author at: Departamento de Física, Universidade Estadual de Ponta Grossa, Av. General Carlos Cavalcanti 4748, 84030-900 Ponta Grossa, PR, Brazil.
E-mail address: eklenzi@dfi.uem.br (E.K. Lenzi).

http://dx.doi.org/10.1016/j.jelechem.2015.03.023
1572-6657/

Our goal is to investigate a PNPA model by considering more than one group of ions. Such study is of great importance for electrolytic cells, such as fuel cells. In particular, liquid crystal cells and displays need to deal with ionic impurities, an undesirable subproduct. It is often necessary to determine the concentration of ions through impedance measurements. Nonetheless, most of the models available do not deal with the reality, which is, to consider more than one ionic impurity, nor do they completely describe the surface effects associated to the confining substrates, all of which contribute to unwelcome characteristics such as low voltage holding ratio. Indeed, generalizations of the PNP model considering different groups of ions have been analyzed before [18–20], but, as discussed above, this approach cannot predict the experimental behavior correctly, specially in the low frequency regime where surface phenomena govern the dynamics. In this article, a model in the PNPA framework considering different groups of ions as well as their valances is reported and compared with experimental data obtained from measuring the impedance spectrum of the mixture of two salts in Milli-Q water: NH_4Cl and $KClO_3$ (both monovalent) $CdCl_2H_2O$ and $HgCl_2$ (both bivalent) in a dilute solutions.

2. The model

Let us introduce an extension of the model proposed in Refs. [9–11] by considering the presence of different groups of positive ($\alpha = +$) and negative ($\alpha = -$) ions in an electrolytic cell of thickness d with electrodes placed at $z = \pm d/2$ of a Cartesian reference frame where z is normal to the electrodes. Thus, we consider the following fractional diffusion equation of distributed order for the bulk densities of ions ($n_{\alpha l}$) in presence of reaction terms $\Lambda_{\alpha l}(t)$

$$\int_0^1 d\gamma' \tau(\gamma') \frac{\partial^{\gamma'}}{\partial t^{\gamma'}} n_{\alpha l}(z,t) = -\frac{\partial}{\partial z} J_{\alpha l}(z,t) - \int_{t_0}^{t} \Lambda_{\alpha l}(t-t') n_{\alpha l}(z,t') dt'. \tag{1}$$

where $\tau(\gamma')$ correspond to a distribution of γ'. Note that depending on the choice of $\tau(\gamma')$ different situations may be recovered such as the the fractional diffusion equation for $\tau(\gamma') \propto \delta(\gamma' - \gamma)$ for $0 < \gamma < 1$, situations characterized by different regimes [21], e.g., $\tau(\gamma') \propto \delta(\gamma' - \gamma) + \tau' \delta(\gamma' - 1), \tau(\gamma') \propto \gamma'^{k-1}$ ultraslow diffusion [22], and for $\tau(\gamma') \propto \delta(\gamma' - 1)$ the usual diffusion is recovered. The current density is given by

$$J_{\alpha l}(z,t) = -\mathcal{D}_{\alpha l} \frac{\partial}{\partial z} n_{\alpha l}(z,t) \mp \frac{q_l \mathcal{D}_{\alpha l}}{k_B T} n_{\alpha l}(z,t) \frac{\partial}{\partial z} V(z,t). \tag{2}$$

In Eq. (2), $\mathcal{D}_{\alpha l}$ and q_l are the diffusion coefficient and the ionic charge of the group l; V is the actual electric potential across a sample, k_B is the Boltzmann constant, and T is absolute temperature. The effective time-dependent potential across the sample is determined by the Poisson's equation

$$\frac{\partial^2}{\partial z^2} V(z,t) = -\frac{1}{\varepsilon} \sum_{l=1}^{N} q_l (n_{+l}(z,t) - n_{-l}(z,t)). \tag{3}$$

In Eq. (3), the dielectric coefficient ε is measured in ε_0 units and N represents the number of different group of ions. We consider that Eq. (1) is subjected to the boundary condition [3,9]

$$J_{\alpha l}\left(\pm\frac{d}{2}, t\right) = \pm \int_0^1 d\vartheta \int_{t_0}^{t} d\bar{t} k_{\alpha l}(t-\bar{t}, \vartheta) \frac{\partial^{\vartheta}}{\partial \bar{t}^{\vartheta}} n_{\alpha l}\left(\pm\frac{d}{2}, \bar{t}\right). \tag{4}$$

The fractional time derivative considered here, in Eqs. (1) and (4), is the Caputo one, given by:

$$\frac{\partial^{\mu}}{\partial t^{\mu}} n_{\alpha l}(z,t) = \frac{1}{\Gamma(1-\mu)} \int_{t_0}^{t} dt' \frac{n'_{\alpha l}(z,t)}{(t-t')^{\mu}}, \tag{5}$$

with $0 < \mu < 1$ and $n'_{\alpha l}(z,t) \equiv \partial_t n_{\alpha l}(z,t)$. Notice this is one of the possible approaches for anomalous diffusion, others scenarios can be found in Ref. [21]. We consider, in Eqs. (1), (4), and (5), $t_0 \to -\infty$ which as discussed in Ref. [23] is suitable choice to analyze the response of the system to a periodic applied potential like the one to be consider here.

Eq. (4) recovers several situations such as the blocking electrodes for $k_{\alpha l}(t,\vartheta) = 0$ ($J_{\alpha l}(z,t)|_{z=\pm\frac{d}{2}} = 0$), adsorption–desorption process at the surfaces corresponding to the Henry approximation (linear kinetic equation of first order) when $k_{\alpha l}(t,\vartheta) \propto e^{-t/\tau}\delta(\vartheta - 1)$, and the Chang-Jaffe condition for $k_{\alpha l}(t,\vartheta) \propto \delta(t)\delta(\vartheta)$ ($J_{\alpha l}(z,t)|_{z=\pm\frac{d}{2}} = \pm k n_{\alpha l}(z,t)|_{z=\pm\frac{d}{2}}$). In this manner, Eq. (4) provides an unified framework for dealing with several boundary conditions and also the non-usual relaxations [24] which emerge when $k_{\alpha l}(t,\vartheta) = \overline{\tau}(\vartheta)\kappa(t)$ for a ϑ distribution $\overline{\tau}(\vartheta)$ and $\kappa(t)$ arbitraries.

The previous set of equations represent a general model for an electrolytic cell containing different groups of ions from which is possible to obtain an analytical solution in the linear approximation for the stationary state and the electrical impedance, as we shall present in the next section.

2.1. Linear approximation

In the linear approximation (small a.c. signal limit), one can consider that $n_{\alpha l}(z,t) = \mathcal{N}_l + \delta n_{\alpha l}(z,t)$, with $\mathcal{N}_l \gg |\delta n_{\alpha l}(z,t)|$, which states that, in the low-voltage regime, the densities differ only slightly from the zero field densities, where $\mathcal{N}_l$ represents the number of ions. In addition, we also consider $\delta n_{\alpha l}(z,t) = \eta_{\alpha l}(z) e^{i\omega t}$ to analyze the impedance when the electrolytic cell is subjected to a time dependent potential $V(z,t) = \phi(z)e^{i\omega t}$, with $V(\pm d/2, t) = \pm V_0 e^{i\omega t}/2$. We also assume that, in each group, the positive and negative ions have the same mobility, i.e., the diffusion coefficients for positive and negative ions of the same group are equal. This assumption avoids cumbersome calculations since the diffusion coefficients are, for the experimental situations analyzed, very similar. The substitution of these expressions into Eqs. (1), (3), and (4) yields a set of coupled equations which may be simplified by using the auxiliary functions $\psi_{\pm l}(z) = \eta_{+l} \pm \eta_{-l}$, where $\psi_{\pm l}(z)$ are solutions of the differential equations

$$\frac{d^2}{dz^2}\psi_{+l} - 2\frac{\mathcal{N}_l}{\mathcal{D}_l}\mathcal{I}_l = \Phi_l(i\omega)\psi_{+l} \tag{6}$$

$$\frac{d^2}{dz^2}\psi_{-l} - \sum_{k=1}^{N} \frac{q_k}{q_l \lambda_l^2}\psi_{-k} = \Phi_l(i\omega)\psi_{-l} \tag{7}$$

where $\Phi_l(i\omega) = \Psi_l(i\omega) + \Lambda_l(i\omega)/\mathcal{D}_l, \Psi_l(i\omega) = (1/\mathcal{D}_l)\int_0^1 d\gamma' \tau(\gamma')(i\omega)^{\gamma'}$, $\Lambda_l(i\omega) = \int_0^{\infty} d\bar{t}\Lambda_l(\bar{t})e^{i\omega\bar{t}}, \mathcal{I}_l = \int_0^{\infty} d\nu \Lambda_l(\nu)$, and $\lambda_l = \sqrt{\varepsilon k_B T/(2\mathcal{N}_l q_l^2)}$ is the Debye screening length. In this scenario, the boundary conditions are given by

$$\frac{d}{dz}\psi_{-l} + 2\frac{q_l \mathcal{N}_l}{k_B T}\frac{d}{dz}\phi\Big|_{z=\pm\frac{d}{2}} = \mp\Upsilon_l(i\omega)\psi_{-l}|_{z=\pm\frac{d}{2}}, \tag{8}$$

$$\frac{d}{dz}\psi_{+l}\Big|_{z=\pm\frac{d}{2}} = \mp\Upsilon_l(i\omega)\psi_{+l}|_{z=\pm\frac{d}{2}}, \tag{9}$$

with $\Upsilon_l(i\omega) = (1/\mathcal{D}_l)\int_0^1 d\vartheta (i\omega)^{\vartheta} \int_0^{\infty} dt' k_{\alpha l}(t',\vartheta) e^{i\omega t'}$.

2.2. Predictions

We consider, for simplicity, the previous system of equations for two group of ions with $q_1 = q_2 = q$, i.e., the same charge, and focus our attention in $\psi_{-l}(z)$ and $\phi(z)$ from which the impedance

can be obtained. Performing some calculation (see the Appendix A) and applying the condition $\phi(z) = -\phi(-z)$ required by the potential, we have that

$$\psi_{-1}(z) = \mathcal{C}_1 \sinh(\delta_1 z) + \mathcal{C}_3 \sinh(\delta_2 z) \tag{10}$$

$$\psi_{-2}(z) = k_1\mathcal{C}_1 \sinh(\delta_1 z) + k_2\mathcal{C}_3 \sinh(\delta_2 z) \tag{11}$$

$$\phi(z) = -\frac{q}{\varepsilon}\left\{\frac{1+k_1}{\delta_1^2}\mathcal{C}_1 \sinh(\delta_1 z) + \frac{1+k_2}{\delta_2^2}\mathcal{C}_3 \sinh(\delta_2 z)\right\} + \mathcal{A}z. \tag{12}$$

Substituting Eqs. (10)–(12) into Eq. (8) and using the condition $\phi(\pm d/2) = \pm V_0/2$ required by the potential the constants $\mathcal{C}_1$ and $\mathcal{C}_3$ can be determined. From these results, it is possible to obtain the electric field $E(z,t)$ and, consequently, the surface density $\Sigma(z,t)$. They are connected by the relation $E(z,t) = -\Sigma(z,t)/\varepsilon = -\partial_z\phi(z)e^{i\omega t}$. In this sense, it is important to note that the current at the electrode is determined by the equation

$$I = \mathcal{S}q\left[(J_{+1}+J_{+2}) - (J_{-1}+J_{-2})\right]_{z=d/2} + \mathcal{S}\frac{\partial}{\partial t}\Sigma\Big|_{z=d/2} \tag{13}$$

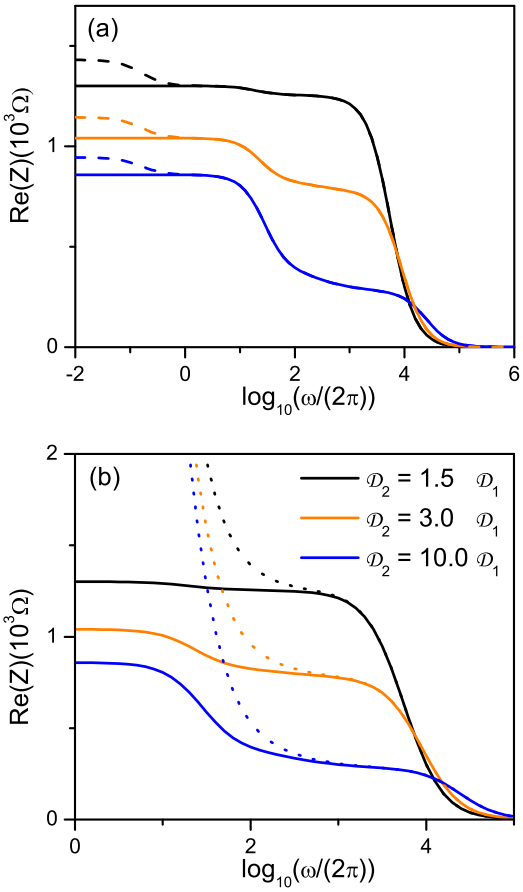

Fig. 1. Behavior of the real part of the impedance for different diffusion coefficients when different boundary conditions are considered. (a) Indicates the cases where perfect blocking electrodes are considered with and without reaction term. The solid lines represents the case $\Lambda_1(i\omega) = \Lambda_2(i\omega) = 0$, for perfect blocking boundary conditions. The reaction term is present in the dashed lines, for which we assumed that $\Lambda_1(i\omega) = \Lambda_2(i\omega) = i\omega/[10(1+i\omega)]$ (as discussed in [25]) for the same boundary conditions. (b) Shows what happens for non-blocking boundary conditions. The dotted lines represents the case $\Lambda_1(i\omega) = \Lambda_2(i\omega) = 0$ for non-blocking boundary conditions while the solid lines are the same curves shown in (a). We consider, for simplicity, $d = 10^{-5}$ m,$\mathcal{S} = 3.14\times10^{-4}$ m^2, $\lambda_1 = \lambda_2 = 2.62\times10^{-7}$ m, $\mathcal{D}_1 = 10^{-9}$ m^2/s,$\tau = 8\times10^{-3}$ s,$\kappa = 4\times10^{-3}$ m/s,$\Phi_l(i\omega) = i\omega/\mathcal{D}_l$, $\nu = 0.5$, and $\varepsilon = 78\varepsilon_0$.

from which the impedance, $Z = V_0e^{i\omega t}/I$, of the electrolytic cell can determined, where $\mathcal{S}$ is the superficial area of the electrode. The current has two contributions as shown in Eq. (13). The first one is directly connected to the boundary conditions and the second is related with electric field produced in the sample by the applied potential difference between the electrodes. For blocking boundary conditions, we have only the contribution of the second part which in the low frequency limit lead us a capacitive behavior, i.e., $Z \sim 1/(i\omega)$. The contribution of the first part is manifested for non-blocking boundary conditions and depends on the choice of $k_{\alpha l}(t)$ and ϑ. In particular, for the situations worked out here, the first part of Eq. (13) plays an important role in the low frequency limit. Futhermore, the model presented here links physicochemical parameters such as diffusion coefficients, number of ions (concentration), kinetic rate parameters (present in the boundary conditions), and sample geometry with experimental impedance measures of impedance.

Fig. 1a illustrates the real part of Z obtained from the previous development when different diffusion coefficients are considered for perfect blocking boundary conditions in absence of the reaction term (solid lines) and in the presence of the reaction term (dotted lines). The real part of the impedance exhibit plateaus that depend on the diffusion coefficients. The larger the difference between the two salts diffusion coefficients become, more pronounced is the presence of a second plateau [19]. When the reaction term is present, another plateau is observed, which is a new result and with implications in systems with generation and recombination of ions. Otherwise, it was shown in Ref. [3] that, in order to obtain a different behavior of the impedance in the low frequency limit, it is necessary to incorporate non-blocking boundary conditions. This point is illustrated in Figs. 1b, 2b, and Fig. 3a and b for the case $\Upsilon_1(i\omega) = \Upsilon(i\omega) = \Upsilon_2(i\omega)$ where $\Upsilon(i\omega) = \kappa\tau(i\omega\tau)^{1-\nu}$ with $0 < \nu < 1$ leading us to a different behavior for the impedance in the low frequency limit which depends on the ν value. In this case,

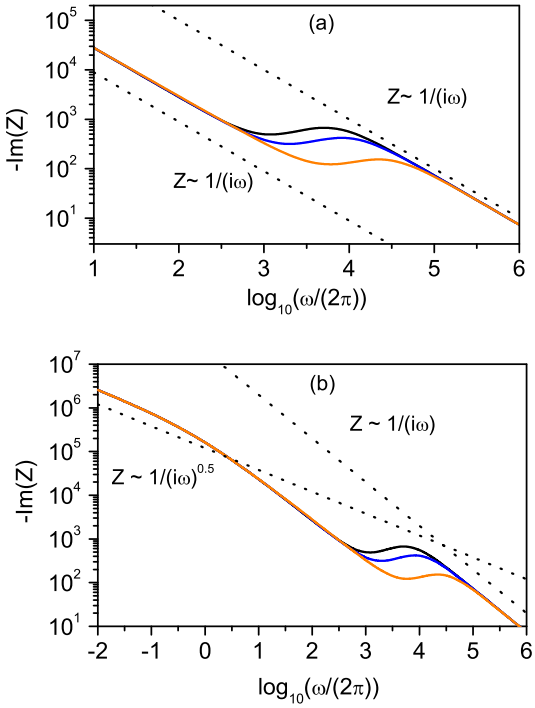

Fig. 2. Behavior of imaginary part of the impedance for different diffusion coefficients when perfect blocking (a) and nonblocking (b) boundary conditions are used. The parameters are the same as for Fig. 1.

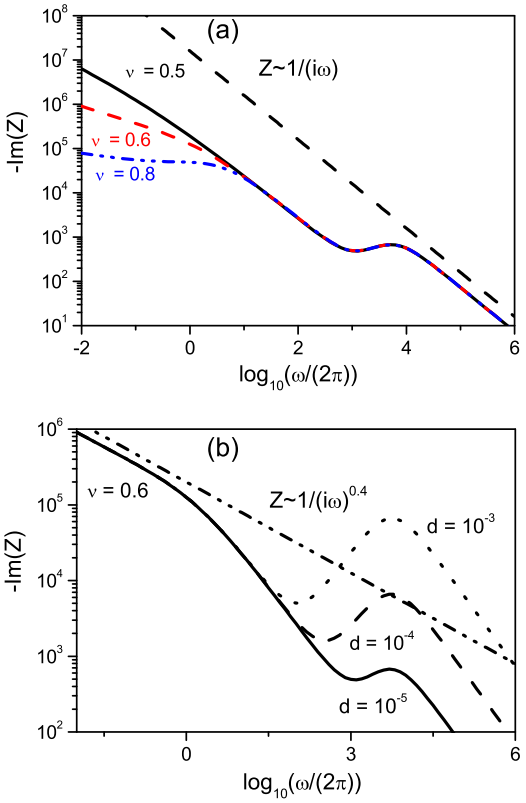

Fig. 3. (a) Shows the behavior of imaginary part of the impedance for different ν values for nonblocking boundary conditions with $\Lambda_1(i\omega) = \Lambda_2(i\omega) = 0, \mathcal{D}_2 = 1.5\mathcal{D}_1$, and $\mathcal{D}_1 = 10^{-9}$ m/s^2. (b) Illustrates the behavior of the imaginary part of the impedance for different thickness in order to show that the behavior in the low frequency limit depends on the boundary conditions, i.e., the electrode surfaces. The others parameters are the same as for Fig. 1. Note that behavior exhibit in the low frequency limit by the impedance depends on the ν value which is connected to the boundary conditions and, consequently, with surface effects.

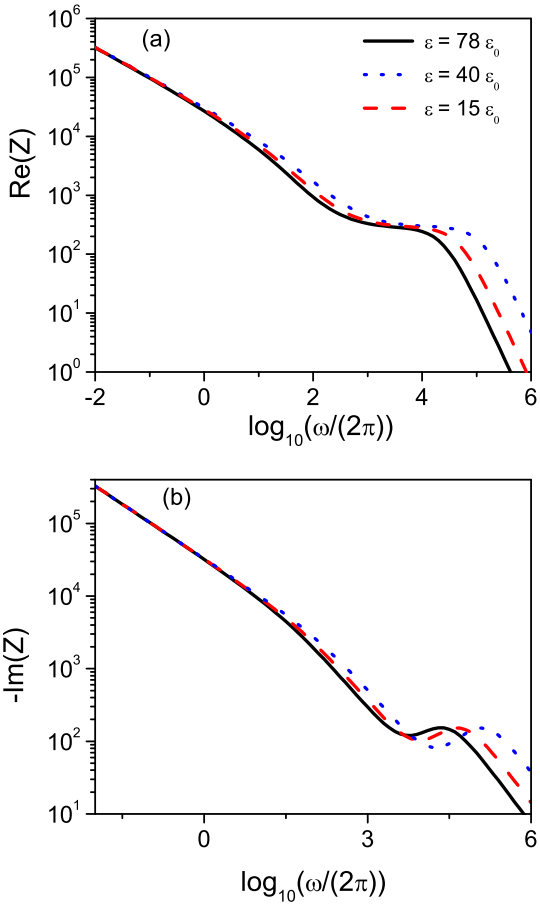

Fig. 4. This figure illustrate the behavior of the real (a) and imaginary (b) parts of the impedance for different values of the ε when nonblocking boundary conditions are considered. We consider, for simplicity, $\mathcal{D}_2 = 10\mathcal{D}_1, \mathcal{D}_1 = 10^{-9}$ m^2/s,$d = 10^{-5}$ m, $\mathcal{S} = 3.14 \times 10^{-4}$ m^2, $\mathcal{N}_1 = \mathcal{N}_2 = 1.5 \times 10^{20}$ m^{-3}, $\tau = 8 \times 10^{-3}$ s,$\kappa = 4 \times 10^{-3}$ m/s, $\Phi_l(i\omega) = i\omega/\mathcal{D}_l$, and $\nu = 0.6$.

the asymptotic behavior of the impedance for $\lambda_1 = \lambda_2 = \lambda$ is given by

$$Z \sim \frac{2\lambda^2}{\varepsilon\mathcal{S}} \frac{1}{(i\omega)\sqrt{2}\lambda + 2\Upsilon(i\omega)} \tag{14}$$

which is independent of the thickness of the sample, depending only on the boundary conditions, i.e., surface effects as shown in Fig. 3b. Thus, the behavior in the low frequency limit is different from the one shown in Fig. 1a and may be connected to surface effects whose kinetic are not governed by a first order equation (Henry isotherm). In fact, the presence of the surface suppresses the second plateau, which seems to be the correct description for experimental systems (see Figs. 2 and 3) and validates our model, with more ingredients in comparison with previously published works [19]. Fig. 4 shows the behavior of the real and imaginary parts of the impedance for different values of ε in order to illustrate the behavior of the drift term. The effect of the different values of ε is more pronounced in the region of high frequency, instead of the region of low frequency. In particular, the behavior in the low frequency limit, i.e., the frequency dependence of the impedance is not influenced as shown by Eq. (14).

2.3. Experimental evidence

Now, we apply the formalism presented in the previous section to investigate the electrical response obtained for different solutions of salt dissolved in Milli-Q deionized water with the dielectric spectroscopy technique. The measurements of the real and imaginary parts of the impedance were performed by using a Solartron *SI* 1296 A impedance/gain phase analyzer. The frequency range used was from 10^{-1} Hz to 10 kHz. The amplitude of the *AC* applied voltage was 20 mV. The ionic solutions were placed into a sample holder – 12962 Solartron between two circular surfaces spaced 1.0 mm from each other. The area of electrodes was 3.14 cm^2. We used electrical contacts made of stainless steel. Before starting the measurements, we adopted the following cleaning procedure: first, the electrodes were washed with detergent and deionized water and then polished with fine sandpaper. Then, the electrodes were placed on an ultrasonic bath for 10 min. The ionic solutions were formed by Milli-Q water mixed with NH_4Cl with $KClO_3$ (concentrations of 4.67×10^{-5} mol L^{-1} and 2.04×10^{-5}mol L^{-1}), both monovalent and $CdCl_2H_2O$ and $HgCl_2$ salts (concentrations of 1.23×10^{-5} mol L^{-1} and 0.91×10^{-5} mol L^{-1}, respectively), both bivalent.

Fig. 5 shows the real and imaginary (inset) parts of the experimental data for both mixtures and the fitting by the model presented here. The agreement for both mixtures is very good when $\Upsilon_l(i\omega) = \kappa_l\tau(i\omega)^{1-\nu_l}$. Notice that, in the low frequency limit, the model presented here is more suitable to describe the experimental data (compare with Fig. 1a, in the perfect blocking situation). In fact, the behavior presented by the experimental data in the low frequency limit is characterized by $Z \sim 1/(i\omega)^{\zeta}$ which can not the obtained from the usual model as previously discussed.

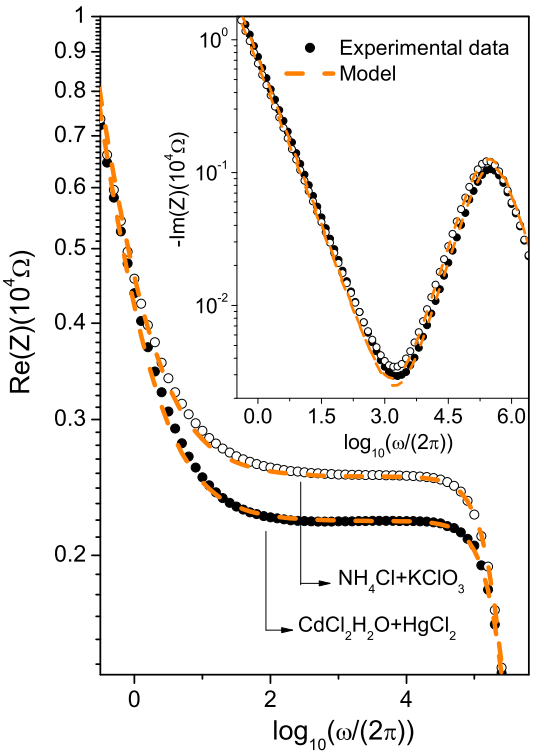

Fig. 5. Measured and best fit impedance (real and imaginary parts) for the two mixtures of salts, involving monovalent and bivalent salts. The fitting was performed with the model presented here. For both measurements, $d = 10^{-3}$ m and $\mathcal{S} = 3.14 \times 10^{-4}$ m^2, come from the experimental setup. We also made $\Phi_l(i\omega) = i\omega/\mathcal{D}_l, \kappa_1 = \kappa_2 = \kappa$ and $\nu_1 = \nu_2 = \nu$ for these cases. For the monovalent salt, $\mathcal{D}_1 = 1.31\mathcal{D}_2 = 5 \times 10^{-9}$ m/s^2, and $\varepsilon = 78\varepsilon_0$ were found in the literature. $\lambda_1 = 1.23\lambda_2 = 7.74 \times 10^{-8}$ m were estimated from the ionic strength (ionic density), since the initial concentrations were known. $\kappa\tau = 7.75 \times 10^{-6}$ m (remember the boundary condition states that $\Upsilon_l(i\omega) = \kappa\tau(i\omega)^{1-\nu}$) and $\nu = 0.21$, were left as fitting parameters. For the bivalent salt, we have $\mathcal{D}_1 = 1.05\mathcal{D}_2 = 4.25 \times 10^{-9}$ m^2/s from the literature, $\lambda_1 = 1.03\lambda_2 = 6.2 \times 10^{-8}$ m estimated from the ionic strength. Then, we have $\kappa\tau = 8.25 \times 10^{-6}$ m, and $\nu = 0.19$ left as fitting parameters.

In particular, for the cases worked out in Fig. 5 the relation between ζ and ν_l is given by $\zeta = 1 - \nu_l$. The parameters used in the fitting are described in the caption of Fig. 5.

These points are an evidence that effects not present in the usual approach, PNP model, have to be incorporated in order to permit a more realistic description of experimental data.

3. Conclusions

We have investigated an extension of the PNPA model by considering the presence of different group of ions. We obtained an analytical solution in the linear approximation and, consequently, the behavior of the impedance by considering two different group of ions. For this case, the ions of the same group have equal diffusion coefficients and ions of different groups have different diffusion coefficient. The results show that the difference between the diffusion coefficients produces another plateau in the low frequency limit when the boundary conditions are characterized by perfect blocking electrodes. Similar behavior is obtained if a linear kinetic equation of first order (Henry isotherm) is considered to describe the adsorption–desorption on the interfaces between electrode and electrolyte. This behavior, in the low frequency limit, is different from the one presented in other approaches where the surface effects are neglected, being observed, for example, in the experimental data of liquid crystal [11,27] and water [26]. These features suggest that the existing effects in the low frequency limit, for the case worked out here, are governed by the interaction between electrode and electrolyte and not by the bulk effects. In order to evidence this feature, we have also compared the predictions of the model presented here with the experimental data obtained from the mixing between two salts with same valence dissolved in Milli-Q water resulting in a good agreement (see Fig. 4). It is worth noticing that the surfaces play a very important role in such systems (which is reflected in the parameter $\nu \neq 1$) and therefore suppress the formation of the second plateau predicted before when surface effects are neglected [19].

Acknowledgments

We would like to thank two anonymous Referees for their reports, both essential to improve the article. We also thanks CNPq (INCT - SC and INCT - FCx) and Fundação Araucária.

Appendix A. Solution for two groups of ions

By solving Eq. (7), the solution obtained for $\psi_{-1}(z)$ and $\psi_{-2}(z)$ is given by

$$\psi_{-1}(z) = \mathcal{C}_1 \sinh(\delta_1 z) + \mathcal{C}_2 \cosh(\delta_1 z) + \mathcal{C}_3 \sinh(\delta_2 z) + \mathcal{C}_4 \times \cosh(\delta_2 z) \tag{15}$$

$$\psi_{-2}(z) = \overline{\mathcal{C}}_1 \sinh(\delta_1 z) + \overline{\mathcal{C}}_2 \cosh(\delta_1 z) + \overline{\mathcal{C}}_3 \sinh(\delta_2 z) + \overline{\mathcal{C}}_4 \times \cosh(\delta_2 z), \tag{16}$$

with

$$\frac{\overline{\mathcal{C}}_1}{\mathcal{C}_1} = \frac{\overline{\mathcal{C}}_2}{\mathcal{C}_2} = \lambda_1^2(\delta_1^2 - \xi_1^2) = k_1 \tag{17}$$

$$\frac{\overline{\mathcal{C}}_3}{\mathcal{C}_3} = \frac{\overline{\mathcal{C}}_4}{\mathcal{C}_4} = \lambda_1^2(\delta_2^2 - \xi_1^2) = k_2, \tag{18}$$

where

$$\delta_{1,2} = \sqrt{\frac{1}{2}(\xi_1^2 + \xi_2^2) \pm \frac{1}{2}\sqrt{(\xi_1^2 - \xi_2^2)^2 + \frac{4}{\lambda_1^2\lambda_2^2}}}, \tag{19}$$

and $\xi_l^2 = 1/\lambda_l^2 + \Phi_l(i\omega)$ (for a general case, see the Appendix B). For the potential, we have that

$$\phi(z) = -\frac{q}{\varepsilon}\left\{\frac{1+k_1}{\delta_1^2}[\mathcal{C}_1 \sinh(\delta_1 z) + \mathcal{C}_2 \cosh(\delta_1 z)] + \frac{1+k_2}{\delta_2^2}[\mathcal{C}_3 \sinh(\delta_2 z) + \mathcal{C}_4 \cosh(\delta_2 z)]\right\} + \mathcal{A}z + \mathcal{B}. \tag{20}$$

In order to find the coefficients, we have to use the boundary condition given by Eq. (8) and the condition required by the potential.

Appendix B. General method

Eq. (7) represents a matrix which, for the case characterized by two ions, has only two lines and two columns. For a more general case, characterized by N ions, this equation can be written in a matrix form as follows:

$$\frac{\partial^2}{\partial z^2}\begin{pmatrix}\psi_{-1}\\ \psi_{-2}\\ \vdots\\ \psi_{-l}\\ \vdots\\ \psi_{-N}\end{pmatrix} = \begin{pmatrix}\xi_1 & \beta_{1,2}^2 & \cdots & \beta_{1,l}^2 & \cdots & \beta_{1,N}^2\\ \beta_{2,1}^2 & \xi_2 & \cdots & \beta_{2,l}^2 & \cdots & \beta_{2,N}^2\\ \vdots & \vdots & \vdots & \vdots & \vdots & \vdots\\ \beta_{l,1}^2 & \beta_{2,l}^2 & \cdots & \xi_l & \cdots & \beta_{l,N}^2\\ \vdots & \vdots & \vdots & \vdots & \vdots & \vdots\\ \beta_{N,1}^2 & \beta_{N,2}^2 & \cdots & \beta_{N,l}^2 & \cdots & \xi_N\end{pmatrix}\begin{pmatrix}\psi_{-1}\\ \psi_{-2}\\ \vdots\\ \psi_{-l}\\ \vdots\\ \psi_{-N}\end{pmatrix} \tag{21}$$

with $\beta_{i,j}^2 = q_j/(q_i\lambda_i^2)$ and $\xi_l^2 = 1/\lambda_l^2 + \Phi_l(i\omega)$. Then the solution to the matrix system of differential equations (21) is given by:

$$\begin{pmatrix} \psi_{-1} \\ \psi_{-2} \\ \vdots \\ \psi_{-l} \\ \vdots \\ \psi_{-N} \end{pmatrix} = \sum_{k=1}^{N} \left\{ \left(\mathcal{C}_{1,k}\cosh(\delta_k) + \mathcal{C}_{2,k}\sinh(\delta_k)\right) \begin{pmatrix} \overline{\xi}_{-1,k} \\ \overline{\xi}_{-2,k} \\ \vdots \\ \overline{\xi}_{-l,k} \\ \vdots \\ \overline{\xi}_{-N,k} \end{pmatrix} \right\} \tag{22}$$

where δ_k is the square root of the kth eigenvalue of the matrix appearing in Eq. (22), while $\overline{\xi}_{-l,k}$ is the lth element of kth eigenvector of the matrix of Eq. (21). Applying the boundary conditions given by Eqs. (8) and (9), the values of the coefficients $\mathcal{C}_{1,k}$ and $\mathcal{C}_{2,k}$ can be obtained.

References

[1] V.F. Lvovchi, Impedance Spectroscopy: Applications to Electrochemical and Dielectric Phenomena, Jonh Wiley & Sons, Hoboken, 2012.
[2] R. Metzler, J. Klafter, Phys. Rep. 339 (2000) 1.
[3] E.K. Lenzi, M.K. Lenzi, F.R.G.B. Silva, G. Gonalves, R. Rossato, R.S. Zola, L.R. Evangelista, J. Electroanal. Chem. 712 (2014) 82.
[4] J. Bisquert, A. Compte, J. Electroanal. Chem. 499 (2001) 112.
[5] J. Bisquert, Phys. Rev. Lett. 91 (2003) 010602.
[6] J. Bisquert, G. Garcia-Belmonte, A. Pitarch, ChemPhysChem 4 (2003) 287.
[7] J. Bisquert, Phys. Rev. E 72 (2005) 011109.
[8] E.K. Lenzi, L.R. Evangelista, G. Barbero, J. Phys. Chem. B 113 (2009) 11371.
[9] P.A. Santoro, J.L. de Paula, E.K. Lenzi, L.R. Evangelista, J. Chem. Phys. 135 (2011) 114704.
[10] E.K. Lenzi, P.R.G. Fernandes, T. Petrucci, H. Mukai, H.V. Ribeiro, Phys. Rev. E 84 (2011) 041128.
[11] F. Ciuchi, A. Mazzulla, N. Scaramuzza, E.K. Lenzi, L.R. Evangelista, J. Phys. Chem. C 116 (2012) 8773.
[12] E.K. Lenzi, J.L. de Paula, F.R.G.B. Silva, L.R. Evangelista, J. Phys. Chem. C 117 (2013) 23685.
[13] J.E.B. Randles, Discuss. Faraday Soc. 1 (1947) 11.
[14] J.R. Macdonald, W.B. Johnson, Fundamentals of impedance spectroscopy, in: E. Barsoukov, J.R. Macdonald (Eds.), Impedance Spectroscopy: Theory, Experiment and Applications, Wiley-Interscience, 2005.
[15] J.R. Macdonald, L.D. Potter Jr., Solid State Ionics 24 (1987) 61.
[16] A. Lasia, Electrochemical impedance spectroscopy and its applications, in: Modern Aspects of Electrochemistry, Kluwer Academic/Plenum Pub, 1999.
[17] J.R. Macdonald, Electroanal. Chem. Interfacial Electrochem. 47 (1973) 182.
[18] J.R. Macdonald, D.R. Franceschetti, J. Chem. Phys. 68 (1978) 1614.
[19] G. Barbero, F. Batalioto, A.M. Figueiredo Neto, Appl. Phys. Lett. 92 (2008) 172908.
[20] A.L. Alexe-Ionescu, G. Barbero, I. Lelidis, J. Phys. Chem. B 113 (2009) 14747.
[21] R. Metzler, J.-H. Jeon, A.G. Cherstvy, E. Barkai, Phys. Chem. Chem. Phys. 16 (2014) 24128.
[22] A.V. Chechkin, R. Gorenflo, I.M. Sokolov, Phys. Rev. E 66 (2002) 046129.
[23] I. Podlubny, Fractional Differential Equations, Academic Press, San Diego, 1999.
[24] E.K. Lenzi, C.A.R. Yednak, L.R. Evangelista, Phys. Rev. E 81 (2010) 011116.
[25] J.L. de Paula, J.A. da Cruz, E.K. Lenzi, L.R. Evangelista, J. Electroanal. Chem. 682 (2012) 116.
[26] E.K. Lenzi, P.R.G. Fernandes, T. Petrucci, H. Mukai, H.V. Ribeiro, M.K. Lenzi, G. Gonçalves, Int. J. Electrochem. Sci. 8 (2013) 2849.
[27] J.L. de Paula, P.A. Santoro, R.S. Zola, E.K. Lenzi, L.R. Evangelista, F. Ciuchi, A. Mazzulla, N. Scaramuzza, Phys. Rev. E 86 (2012) 051705.